Two Competing Mechanisms for the Copper-Free Sonogashira Cross-Coupling Reaction

Thomas Ljungdahl, Timmanna Bennur, Andrea Dallas, Hans Emtenäs,[†] and Jerker Mårtensson*

Department of Chemical and Biological Engineering/Organic Chemistry, Chalmers University of Technology, SE-412 96 Göteborg, Sweden

Received March 18, 2008

The mechanism of the copper-free Sonogashira cross-coupling was investigated using a model reaction with differently *para*-substituted phenylacetylenes and 4-iodobenzotrifluoride as coupling partners and a $Pd_2(dba)_3 \cdot CHCl_3-AsPh_3$ catalyst system in methanol. A carbopalladation mechanism was ruled out through a series of experiments in which the equivalent of a carbopalladation reaction intermediate was synthesized by an alternate route, and its conversion to product was monitored. A Hammett correlation study revealed a possible mechanistic changeover when going from electron-rich to electron-poor alkynes in the model reaction. It is advocated that the reaction mechanism changes from a pathway involving a fast proton transfer from a slowly forming cationic Pd complex to a pathway involving a slow proton transfer from a neutral Pd complex on going from electron-rich to electron-poor alkynes. The amine base is believed to act as a base in both pathways and as a nucleophile promoting the formation of the cationic complex in the reactions involving electron-rich alkynes. This was substantiated by the observation of a primary isotope effect ($k_{Alkyne\text{-}H}/k_{Alkyne\text{-}D} \approx 2$) for the electron-poor alkyne and a pronounced base dependence for the electron-rich one.

Introduction

The palladium-catalyzed cross-coupling of a terminal alkyne with a vinyl or aryl halide is a powerful reaction in organic synthesis because it provides a direct route to $sp-sp^2$ carbon−carbon bonds.[1–3] In the presence of cuprous iodide, the reaction is known as the Sonogashira reaction.[4] Since the discovery of the copper-assisted reaction by Sonogashira in 1975, it has found wide applications in the synthesis of such diverse areas as molecular wires,[5] nonlinear optics,[6] natural products,[7] and steroid analogues.[8] The copper additive, however, may be detrimental to the reaction outcome for some substrates and under certain circumstances.[9–11] To address this problem, copper-free conditions have also been developed, thus increasing the reaction scope even further. The reaction under such conditions is known either as the Heck alkynylation[12–14] or as a copper-free Sonogashira reaction,[15–18] depending on the exact conditions, the substrates, and the author.

Although the literature is scarce in details regarding the mechanism of the Sonogashira reaction,[19] a generally accepted notion seems to be that the catalytic cycle features the typical steps of a palladium-catalyzed cross-coupling, i.e., oxidative addition,[20,21] transmetalation,[22,23] and reductive elimination.[24,25] This was also what was suggested in the original publication.[4] Without the involvement of copper there are even fewer mechanistic suggestions to be found. Two mechanistic pathways seem feasible, but are often described in vague terms. They both share an initial oxidative addition and alkyne coordination, but while one of them is completed by subsequent deprotonation and reductive elimination, the other involves consecutive

* Corresponding author. Fax: +46 (0)31 772 36 57. E-mail: jerker@chalmers.se.

[†] Astra Zeneca R&D Mölndal, Sweden.

(1) Sonogashira, K. *J. Organomet. Chem.* **2002**, *653*, 46.
(2) Negishi, E.; Anastasia, L. *Chem. Rev.* **2003**, *103*, 1979.
(3) Tykwinski, R. R. *Angew. Chem., Int. Ed.* **2003**, *42*, 1566.
(4) Sonogashira, K.; Tohda, Y.; Hagihara, N. *Tetrahedron Lett.* **1975**, *16*, 4467.
(5) Hortholary, C.; Coudret, C. *J. Org. Chem.* **2003**, *68*, 2167.
(6) Raimundo, J.-M.; Lecomte, S.; Edelmann, M. J.; Concilio, S.; Biaggio, I.; Bosshard, C.; Günter, P.; Diederich, F. *J. Mater. Chem.* **2004**, *14*, 292.
(7) Myers, A. G.; Tom, N. J.; Fraley, M. E.; Cohen, S. B.; Madar, D. J. *J. Am. Chem. Soc.* **1997**, *119*, 6072.
(8) Donets, P. A.; Latyshev, G. V.; Lukashev, N. V.; Beletskaya, I. P. *Russ. Chem. Bull.* **2007**, *56*, 504.
(9) Wagner, R. W.; Johnson, T. E.; Li, F.; Lindsey, J. S. *J. Org. Chem.* **1995**, *60*, 5266.
(10) Ljungdahl, T.; Pettersson, K.; Albinsson, B.; Mårtensson, J. *J. Org. Chem.* **2006**, *71*, 1677.
(11) Wagner, R. W.; Ciringh, Y.; Clausen, C.; Lindsey, J. S. *Chem. Mater.* **1999**, *11*, 2974.
(12) Dieck, H. A.; Heck, F. R. *J. Organomet. Chem.* **1975**, *93*, 259.
(13) Hierso, J.-C.; Boudon, J.; Picquet, M.; Meunier, P. *Eur. J. Org. Chem.* **2007**, 583.
(14) Boukouvalas, J.; Côté, S.; Ndzi, B. *Tetrahedron Lett.* **2007**, *48*, 105.
(15) Leadbeater, N. E.; Tominack, B. J. *Tetrahedron Lett.* **2003**, *44*, 8653.
(16) Kim, J.-H.; Lee, D.-H.; Jun, B.-H.; Lee, Y.-S. *Tetrahedron Lett.* **2007**, *48*, 7079.
(17) Soheili, A.; Albaneze-Walker, J.; Murry, J. A.; Dormer, P. G.; Hughes, D. L. *Org. Lett.* **2003**, *5*, 4191.
(18) Cheng, J.; Sun, Y.; Wang, F.; Guo, M.; Xu, J.-H.; Pan, Y.; Zhang, Z. *J. Org. Chem.* **2004**, *69*, 5428.
(19) Jutand, A. *Pure Appl. Chem.* **2004**, *76*, 565.
(20) Amatore, C.; Pflüger, F. *Organometallics* **1990**, *9*, 2276.
(21) Casado, A. L.; Espinet, P. *Organometallics* **1998**, *17*, 954.
(22) Osakada, K.; Hamada, M.; Yamamoto, T. *Organometallics* **2000**, *19*, 458.
(23) Ogawa, H.; Onitsuka, K.; Joh, T.; Takahashi, S.; Yamamoto, Y.; Yamazaki, H. *Organometallics* **1988**, *7*, 2257.
(24) Komiya, S.; Albright, T. A.; Hoffmann, R.; Kochi, J. K. *J. Am. Chem. Soc.* **1976**, *98*, 7255.
(25) Osakada, K.; Sakata, R.; Yamamoto, T. *Organometallics* **1997**, *16*, 5354.

10.1021/om800251s CCC: $40.75
Publication on Web 05/02/2008

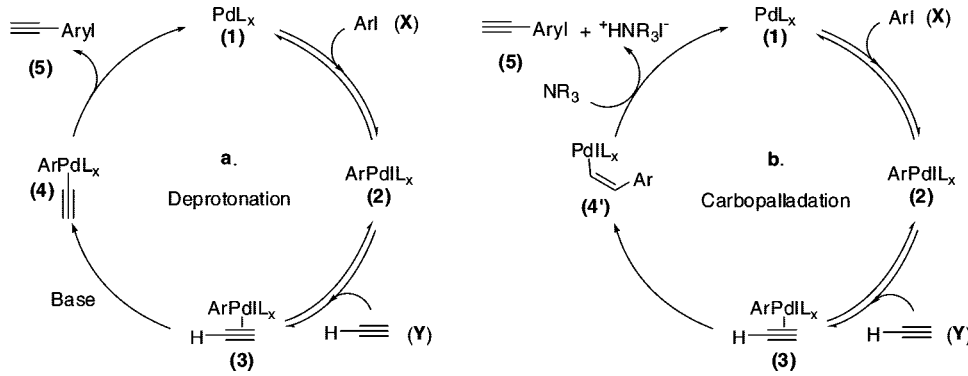

Figure 1. Mechanism for palladium-catalyzed copper-free cross-coupling between a terminal alkyne and an aryl halide as proposed by (a) Soheili[17] and (b) Heck.[12]

carbopalladation and hydride elimination.[12,26,27] The catalytic cycle for a deprotonation-type mechanism, as proposed by Soheili et al.,[17] featured some form of deprotonation/reductive elimination sequence as the key step and can be seen to the left in Figure 1. The catalytic cycle to the right in the same figure depicts a hypothetical carbopalladation mechanism.

The two catalytic cycles actually have the two first steps in common: The catalytically active species **1**, at which the catalytic cycle commences, can be of colloidal nature and/or low-ligated Pd^0-species stabilized by the ligands present, including the base and/or solvent molecules. In the first step the catalytic cycle is initiated by oxidative addition of the aryl or vinyl halide to species **1**, forming the oxidative addition adduct **2** as a homogeneous Pd^{II} species. The following second step is a reversible coordination of the alkyne **Y** to **2**, which produces an alkyne−Pd^{II} complex **3**. In the deprotonation-type mechanism the base then removes a proton from the coordinated alkyne, forming the palladium−acetylide complex **4**, from which the cross-coupled product **5** is expelled and species **1** re-formed by reductive elimination. In the carbopalladation-type mechanism, on the other hand, the Pd−Ar complex coordinated to the alkyne is added over the triple bond, forming complex **4′**, and the cross-coupled product **5** is then expelled and species **1** re-formed through β-hydride elimination.

We have previously reported that particularly efficient copper-free reaction conditions for sensitive porphyrin substrates can be achieved using a highly polar solvent together with a tertiary unhindered amine for a $Pd_2(dba)_3 \cdot CHCl_3/AsPh_3$ catalyst system.[10] This previous study focused on the importance of the solvent and the base to the reaction as opposed to focusing on the role of the ligand, which has been a more common approach to reaction optimization. To explain the observed trends in solvent and base dependence, the overall rate for the catalytic cycle was proposed to be determined by the deprotonation step, featuring a transition state with significant charge separation.

Herein, we aim to provide more detailed information about the mechanistic aspects of this reaction. We commence with a presentation and discussion of experimental evidence that disprove a plausible carbopalladation mechanism as the actual reaction pathway. Other possible mechanistic pathways, supported by data presented, are then detailed. A Hammett correlation study follows, which indicates that there is a switch in reaction mechanism when changing from electron-rich to electron-poor alkyne substrates. The proposed competition between two mechanisms is then further substantiated by an account of the observed kinetic isotope effects and also by a discussion of the changes in observed base dependence of the reaction for different substrates.

Scheme 1. Alternate Route to and the Trapping of the Proposed Carbopalladation Intermediate

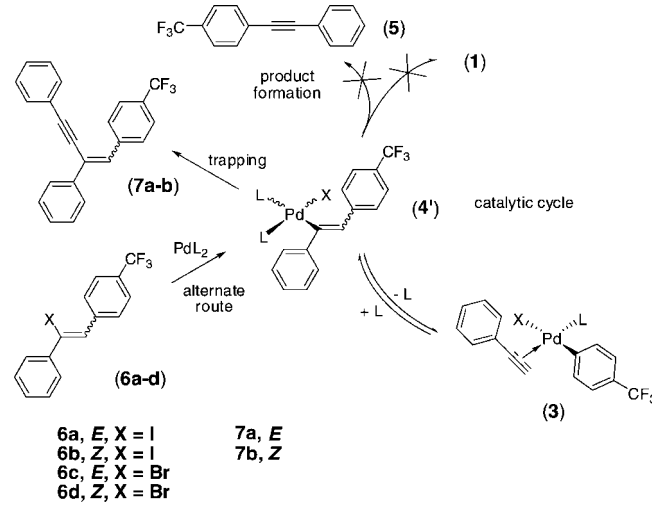

Results and Discussion

Carbopalladation. In the literature a carbopalladation mechanism has in some cases been invoked to explain how the copper-free Sonogashira couplings occur.[12,26] An experiment to test whether a carbopalladation mechanism was likely to explain the product formation under the given reaction conditions was devised. In this investigation, a Pd complex of **4′** type (see Figure 1 and Scheme 1) was synthesized via the oxidative addition of a halostilbene (**6**), and product formation was monitored under experimental conditions similar to those of the model reaction used in the further mechanistic studies (*vide infra*).

The stereochemistry of the intermediate **4′** is based on the generally accepted notion of a *syn*-migration of the palladium complex and the benzotrifluoride moiety to give the *Z*-isomer with the new aryl group transferred to the less hindered position.[26] This intermediate was synthesized in methanol directly from the corresponding halostilbene (**6**) and equimolar amounts of the same catalyst as for the model reaction. The experiments were performed in the absence of base to check for intramolecular β-hydride elimination and with base (NEt_3, 100 equiv) to check for base-assisted *trans*-elimination. To make

(26) Amatore, C.; Bensalem, S.; Ghalem, S.; Jutand, A. *J. Organomet. Chem.* **2004**, *689*, 4642.
(27) Negishi, E. I.; Copéret, C.; Ma, S.; Liou, S.-Y.; Liu, F. *Chem. Rev.* **1996**, *96*, 365.

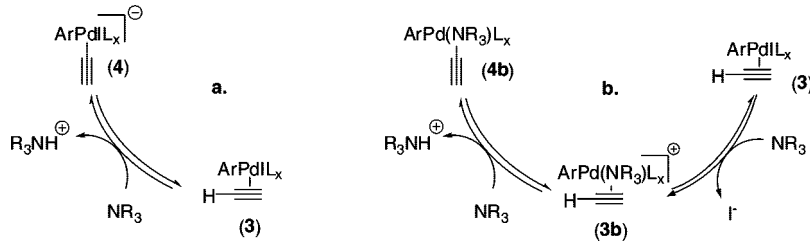

Figure 2. Proposed (a) anionic pathway and (b) cationic pathway.

sure that an unexpected *E*-isomer was not the intermediate and responsible for product formation by more facile intramolecular β-hydride elimination, the reaction was performed for both the *Z*- and *E*-isomers.

Oxidative addition clearly took place, albeit with different rates depending on the halide and the isomer of the halostilbene (**6**). This was established through the disappearance of the starting material and the appearance of a multitude of CF_3-containing species in the ^{19}F NMR spectrum. It was also confirmed by trapping experiments with phenylacetylene to produce the cross-coupled ene-yne products **7**. However, no elimination to produce 4-trifluoromethyltolane could be detected in any of the experiments. This is in marked contrast to the facile formation of tolane **5** under similar conditions from the 4-iodobenzotrifluoride and phenylacetylene. It was therefore concluded that carbopalladation is not operative under the reaction conditions applied in the present study (for details and representative spectra see the Supporting Information).

Mechanistic Hypothesis: Anionic versus Cationic Pathways. With the carbapalladation rejected as the operative mechanism under the topical reaction conditions, the actual mechanism is more likely, as proposed by Soheili et al., of the deprotonation−reductive elimination type. This assumption is corroborated by the previous study of solvent and base dependencies[10] and by the current results (*vide infra*). More specifically, based on the experimental results presented, we propose two possible mechanistic pathways for the deprotonation. Either a direct deprotonation of alkyne−palladium complex **3** into palladium−acetylide complexes **4** or transformation of alkyne−palladium complex **3** into complex **4b** via a ligand exchange−deprotonation sequence (see Figure 2).

Crucial to the first reaction sequence (a) is the activation of the alkyne toward base-assisted proton removal by coordination to the oxidative addition adduct **2** (Figure 1). Subsequent coordination of the alkyne, the palladium−acetylide complex **4** is formed in a single step concurrently with the base-assisted proton removal. Despite activation, the proton transfer step is a very slow reaction step and determines the rate of the catalyzed reaction. If the iodide were to be expelled concomitant with proton abstraction, complex **4** would be uncharged. However, more likely than the formation of a coordinatively unsaturated tricoordinate neutral complex seems to be the formation of a negatively charged coordinatively saturated palladate complex, at least as an initial intermediate. In the second reaction sequence (b) the activation of the alkyne toward base-assisted proton removal is too weak for immediate proton transfer to compete successfully. An additional step has to precede the proton transfer to achieve sufficient activation of the alkyne toward base attack. This step is a base-assisted formation of a cationic palladium complex, in which the anionic halide is exchanged for the neutral base (amine) as ligand on the palladium. Amines have been shown to be excellent ligands for palladium(II), competing successfully with ligands such as arsines and phosphines.[28] Furthermore, formation of cationic palladium complexes has been shown to be important for the overall efficiency under certain reaction conditions for several other catalytic processes, e.g., for the Heck coupling,[29–31] the Stille coupling,[32] and palladium-catalyzed nucleophilic additions to olefins.[33] After base−halide exchange, the more electron-deficient palladium center of the cationic complex is proposed to have a sufficient activation capability to support the required proton transfer. In fact, the efficient activation leads to a rapid proton transfer compared to the rate of formation of the cationic palladium complex, which in this case becomes the rate-determining step of the catalytic cycle.

The viability of the two proposed mechanisms was compared by a limited computational study. The relative energies of the equilibrium geometries *in vacuo* of selected intermediate palladium complexes for the two proposed pathways were calculated at the B3LYP/LANLDZ level (see the Supporting Information for details about the calculations). The relative energies, shown graphically in Figure 3, indicate that the initial steps of the two competing reaction pathways are both highly endergonic and of similar magnitude.

Further, the reaction energies depend strongly on electronic factors, as explored by calculations on systems formed from alkynes substituted with either electron-donating (EDG) or electron-withdrawing (EWG) groups. The energy of reaction for the proton transfer from the iodo complex **3** is 19.5 kcal/mol less endergonic for the electron-deficient nitro complex than for the electron-rich dimethylamino analogue. In contrast, the iodide−base exchange for the competing reaction pathway is 14.6 kcal/mol more endergonic for the nitro complex compared to the dimethylamino analogue. Thus, the substituent effect works in opposing directions for the two reaction pathways; the energy of reaction for the proton transfer is decreased by the electron-withdrawing group and increased by the electron-donating one, whereas the contrary is true for the iodide−base exchange reaction. This indicates that the preferred pathway may vary with substrate. However, the approximate nature of the computational study should be kept in mind. Especially the solvent effects, not accounted for in the calculations, could have a large impact on the reaction.

The proposed mechanisms were derived from the result of a series of experiments based on a model reaction, i.e., the coupling of 4-iodobenzotrifluoride and phenylacetylene in the presence of triethylamine (TEA) and $Pd_2(dba)_3 \cdot CHCl_3/AsPh_3$

(28) Tougerti, A.; Negri, S.; Jutand, A. *Chem.−Eur. J.* **2007**, *13*, 666.
(29) Cabri, W.; Candiani, I. *Acc. Chem. Res.* **1995**, *28*, 2.
(30) Cabri, W.; Candiani, I.; DeBernardinis, S.; Francalanci, F.; Penco, S.; Santi, R. *J. Org. Chem.* **1991**, *56*, 5796.
(31) Ozawa, F.; Kubo, A.; Hayashi, T. *J. Am. Chem. Soc.* **1991**, *113*, 1417.
(32) Espinet, P.; Echavarren, A. M. *Angew. Chem., Int. Ed.* **2004**, *43*, 4704.
(33) Åkermark, B.; Almemark, M.; Almlöf, J.; Bäckvall, J. E.; Roos, B.; Støgard, Å. *J. Am. Chem. Soc.* **1977**, *99*, 4617.

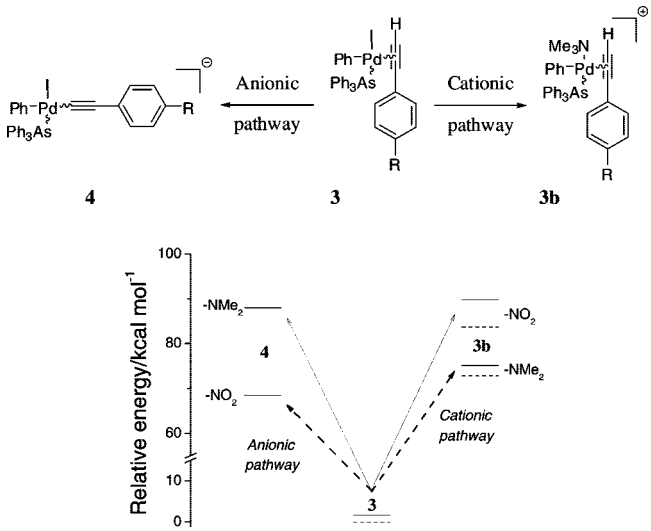

Figure 3. Relative energies calculated at the B3LYP/LANLDZ level for the first intermediate (**3b** or **4**; R = $-NMe_2$ or $-NO_2$) along each of the two reaction pathways. Solid lines (—) indicate the relative energies of configurations related to the [*SP*-4-3] isomer (for naming of stereoisomers, see the Supporting Information) of the alkyne-coordinated oxidative addition adduct, and dashed lines (- - -) the energies of the corresponding [*SP*-4-2] complexes. The energies are shown relative to that of the [*SP*-4-2] complex of the alkyne-coordinated oxidative addition adduct **3**. Both the electron-rich Me_2N and the electron-poor NO_2 analogue of the respective isomer of complex **3** are arbitrarily assigned the same energy.

with methanol as the solvent.[10] The choice of this aryl halide is based on the assumption that the activating effect of the trifluoromethyl group in the oxidative addition should prevent this step from becoming rate determining, thus allowing us to focus more on the deprotonation/insertion step. The trifluoromethyl group is also a reporter group that enables the reaction progress to be monitored by ^{19}F NMR spectroscopy (see the Supporting Information for further details). The results of these studies are discussed in the following paragraphs.

Hammett Correlation Studies. To provide more information about the rate-limiting step in the catalytic cycle, Hammett correlation studies were performed. The required rate ratios, k_R/k_H, were obtained experimentally in two ways: either from a series of competitive reactions, in which equimolar concentrations of phenylacetylene and one of its *para*-substituted derivatives were reacted with 4-iodobenzotrifluoride, or from a series of reactions with a single phenylacetylene derivative in each reaction; see Scheme 2.

The reactions were performed directly in the NMR tubes, and the progress of the reactions was monitored by recording the integrals corresponding to the formed cross-coupling product and the consumed aryl halide every 5 min.

The initial rates r_H and r_R were calculated as the first derivative at time zero of the regression equations found by fitting of a monoexponential function ($y = A\ \exp(-t_1/x) - y_0$) to the kinetic data. Although somewhat arbitrary, the choice of a monoexponential function can be justified on the basis of a simple kinetic three-state model: an initial and irreversible formation of the oxidative addition adduct followed by a reversible formation of an acetylide complex, and a final irreversible formation of tolane and the palladium(0) species via reductive elimination. The unknown unimolecular processes intervening between the oxidative addition adduct and the complex from which the product is formed by reductive elimination are combined in a single step, characterized by the overall kinetic constants for the forward and the reverse process. Applying the steady-state approximation for the three species and assuming that the formation of the acetylide complex is the rate-determining step yields a first-order rate expression (for details see the Supporting Information). This expression corresponds to a monoexponential increase in the tolane concentration with increasing reaction time. Indeed, the increase in concentration of tolane followed an approximate monoexponential time course.

Scheme 2. Reaction Systems Used in the Hammett Studies[a]

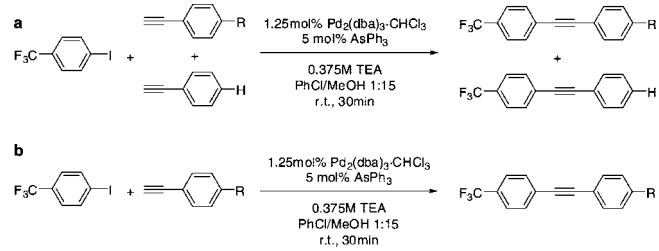

[a] (a) The reaction system used for the competitive studies; R = NMe_2, OMe, Me, Cl, Ac, or NO_2. The reactant concentrations were 0.0125 M in 4-iodobenzotrifluoride and 0.00625 M in each alkyne. (b) The reaction system used for the absolute rate determinations; R = NMe_2, OMe, H, Ac, or NO_2. The concentration was 0.0125 M for both reactants.

The competitive studies were in part carried out because of the poor stability of the precatalyst in its stock solution. The activity of the catalyst diminished slowly during the period required to measure the rates for the full series of reaction systems. More accurate measures of the rate ratios were expected from the competitive experiments because the reaction rates for both the substituted and the unsubstituted phenylacetylenes were measured under exactly the same reaction conditions, independent of aging of the stock solution and other small variations in experimental parameters. Another advantage of the competitive reactions is that the effect on the reaction step(s) intended for scrutiny is refined. The effects of differences in other processes caused by the substituent effect are eliminated or decreased. One such effect is the shift in the equilibrium composition between the catalytically active palladium(0) species and its unreactive alkyne-complexed counterpart (see section 4.3, Supporting Information).[34] Irrespectively of variations in such processes, both the substituted and the unsubstituted alkyne will experience the same concentration of oxidative addition adduct during the reaction. From this intermediate and onward back to the initial palladium(0) species, the two catalytic cycles will proceed with their respective substituent-specific rate constants (for details see the Supporting Information).

Both single alkyne and competitive reactions were conducted and analyzed. The data and resulting Hammett plots obtained from the two series of experiments are very similar, but the ones from the competitive experiments were obtained with slightly higher precision. The logarithm of the ratio between the initial cross-coupling rate of the substituted alkyne and the one for phenylacetylene was plotted versus the Hammett substituent constants; see Figure 4.

The overall shape of the Hammett curves indicates that there is a mechanistic changeover going from electron-donating to electron-withdrawing substituents at the *para* position on the phenylacetylene substrates. The mechanistic changeover seems to occur quite abruptly at $\sigma_i \approx 0$. The left section shows a linear

(34) Amatore, C.; Bensalem, S.; Ghalem, S.; Jutand, A.; Medjour, Y. *Eur. J. Org. Chem.* **2004**, 366.

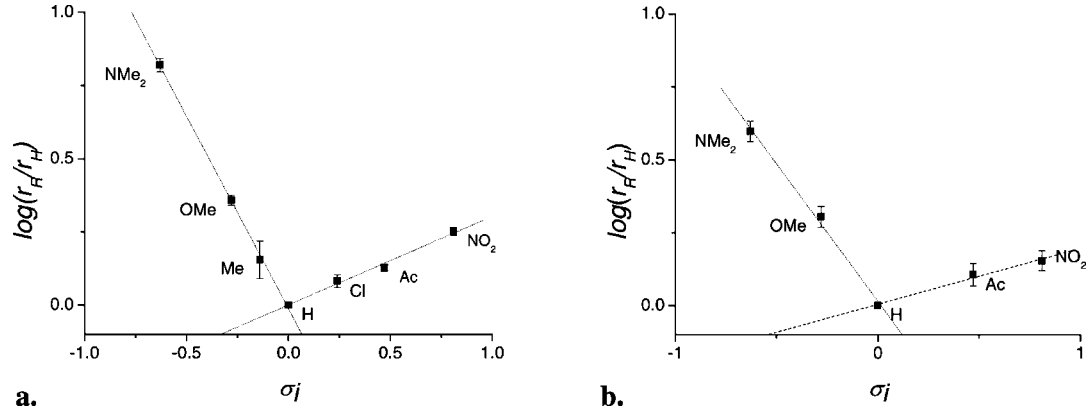

Figure 4. Hammett plot for the alkynylation reaction based on data from (a) competitive studies and (b) noncompetitive studies. The indicated errors in graph a are the standard deviation in the logarithm of the quotient between the initial reaction rates obtained in the competitive studies. The errors in graph b are based on the standard deviations in the estimated initial rates for the coupling reactions of the substituted and unsubstituted reactants.

correlation between $\log(r_R/r_H)$ and the substituent constant σ_i with a negative reaction parameter ρ. Such a negative ρ value is usually indicative of a decrease in electron density at the reaction center in the transition state of one or more reaction steps in the reaction, here on the path from oxidative addition adduct to the tolane and the palladium(0) species. The right-hand section on the other hand shows a linear correlation with a small positive value, indicative of an increase in electron density at the reaction center of one or more steps. However, it is not possible to make any exact mechanistic statements from the Hammett data. In a multistep reaction sequence, such as the present reactions, several or all of the individual steps involved may contribute to the observed ρ value. Furthermore, a complete kinetic model would presumably lead to a complicated rate equation for which there is no simple and transparent approximate expression that could provide mechanistic insight. Even for the expression for the relative reactivity of the substituted substrates derived from a simple kinetic four-state model there is no simple and transparent approximation (for details see section 4.3, equation S37 in the Supporting Information).

In spite of the difficulty to deconvolute an observed reaction rate for a metal-catalyzed reaction into rates for the individual elementary steps, Hammett studies have in different contexts proven to be a valuable tool to gain, at least qualitatively, insight into the mechanism of such reactions.[35–38]

The carbopalladation−elimination sequence in the Heck reaction has been shown to occur via cationic palladium complexes under specific reaction conditions. Similarly, an analogous pathway could be invoked for the copper-free Sonogashira reaction to account for the negative ρ value observed for the electron-donating substituents under the present reaction conditions. Located within the mechanistic changeover region, cross-coupling of phenylacetylene is likely to proceed via both possible mechanisms, accounting for the negative and the positive ρ values, respectively. However, the vinylpalladium complex **4′**, prepared in the carbopalladation study, does not yield the expected tolane **5**, although this is readily formed in the normal copper-free Sonogashira reaction from the 4-iodobenzotrifluoride and phenylacetylene under similar conditions (*vide supra*). Thus, a different mechanistic pathway than the carbopalladation−elimination sequence must be operative for the electron-rich substrates.

Although no exact mechanistic statements can be given, the observed negative ρ value for the electron-donating substituents agrees with the proposed rate-limiting formation of a cationic palladium complex prior to the proton transfer and acetylide complex formation. Furthermore, the observed positive ρ value for the electron-withdrawing substituents corroborate the hypothesized rate-limiting proton transfer from an acetylene−palladium(II) complex.

Base Dependence−Substrate Correlation. Regardless of whether the anionic or the cationic mechanisms dominate under the experimental conditions, the reaction should show a dependence on the concentration of the base. Indeed, a linear increase in reaction rate with increased base concentration was observed for the cross-coupling reaction. However, a decrease in the rate was obvious when the amine was used in large excess, thus indicating that some sort of deactivation/competitive coordination occurred at higher amine concentrations (see Figure S10 in the Supporting Information). It has previously been shown that at high concentrations triethylamine reversibly forms the less reactive species of the type $[ArPdX(AsPh_3)(amine)]$ generated by the reaction of amines with *trans*-$[ArPdX(AsPh_3)_2]$ complexes.[13] Alternatively, the decrease in reaction rate could be explained by the strongly decreased solvating power of the solvent when it consists to a large degree of the nonpolar amine rather than the very polar MeOH. The solvating power has been shown to be very important in our previous work on this reaction. Nevertheless, it has been observed that the choice of amine concentration should be carefully decided and that more is not always better.

If two different mechanisms were in operation depending on the nature of the alkyne, there should most likely be a difference in their base dependencies. Therefore, the differences in the base dependencies between phenylacetylenic substrates substituted with an electron-withdrawing group and an electron-donating group was explored. In the suggested cationic mechanism, operative with EDG-substituted substrates, the role of the amine is primarily to form a cationic complex such as $[ArPdL_x(amine)_x]^+$ in a ligand-substitution reaction.[39,40] Thus, the nucleo-

(35) Muñiz, K.; Hövelmann, C. H.; Streuff, J. *J. Am. Chem. Soc.* **2008**, *130*, 763.
(36) Liang, L.-C.; Chien, P.-S.; Huang, M.-H. *Organometallics* **2005**, *24*, 353.
(37) Constantine, R. N.; Kim, N.; Bunt, R. C. *Org. Lett.* **2003**, *5*, 2279.
(38) Qu, Z.; Shi, W.; Wang, J. *J. Org. Chem.* **2001**, *66*, 8139.
(39) Cusumano, M.; Faraone, G.; Ricevuto, V.; Romeo, R.; Trozzi, M. *J. Chem. Soc., Dalton Trans.* **1974**, 490.

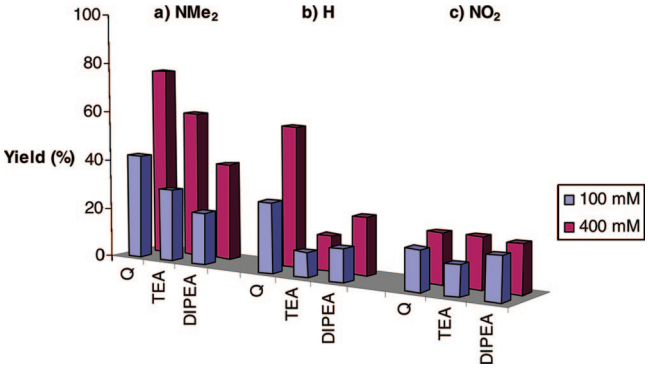

Figure 5. Conversion after 1 h for different substrate−base combinations. Reactions run at the lower concentrations of base are shown in front.

philicity of the base should be the most important property for the reactions involving phenylacetylenes substituted by electron-donating groups.[41,42] For the EWG-substituted alkynes, for which the deprotonation mechanism is believed to be the most important, the base strength should probably be the property of importance.

To probe the dependence on the nature of the base, the reaction conditions applied in the model reaction were adjusted somewhat. The dependence was studied by measuring the changes in conversion for a set of reactions carried out with differently substituted phenylacetylenes in the presence of varying bases. To ensure that any differences in conversion between the reactions were clearly discernible, a relatively low reaction conversion for all substrates was certified by a lowering of the palladium loading to 0.4 mol %. The reaction time was increased to 1 h to minimize the effects of the handling of the reactions. The bases chosen were quinuclidine (Q), triethylamine (TEA), and diisopropylethylamine (DIPEA), for which there is a marked increase in steric hindrance, in the order Q < TEA < DIPEA.[43,44] The alkyne substrates were NMe_2- and NO_2-substituted phenylacetylenes (4-ethynyl-*N*,*N*-dimethylaniline and 1-ethynyl-4-nitrobenzene), with phenylacetylene included as a control. The bases were added at concentrations of 100 and 400 mM, which correspond to 10 and 40 equiv of base relative to the coupling partners. The yields of the reactions were monitored by ^{19}F NMR spectroscopy after quenching the reactions with 1,2-bis(diphenylphosphino)ethane (dppe). The results are shown in Figure 5.

At these concentrations, the reaction rate was the fastest for the NMe_2-substituted phenylacetylene and slowest for the NO_2-substituted phenylacetylene. More importantly, a much more pronounced dependence on the concentration and nature of the base is seen for the NMe_2-substituted phenylacetylene, whereas very little base dependence is seen for the NO_2-substituted phenylacetylene. The unsubstituted phenylacetylene is apparently a cross between these two outcomes.

The dependence of reaction conversion for the EDG-substituted phenylacetylene on the nature of the amine indicates that the less sterically hindered and most nucleophilic base quinuclidine is the most effective. The nucleophilicity of an amine can be estimated through a combination of its cone angle[43,44] and the vertical ionization potential (IE_v).[10,45–49] Here the IE_vs are similar for all three amines, which is why the cone angle will be the determining factor. The observed base dependencies strengthen the hypothesis that the base plays the role of a nucleophile and that a cationic intermediate species is formed when EDG-substituted phenylacetylenes are used.

On the other hand, the electron-poor phenylacetylene shows almost no dependence on the nature of the base and very little dependence on the base concentration. This suggests that the base plays a different role for electron-poor substrates compared to electron-rich ones. A possibility is that the EWG activates the alkyne sufficiently for a fast deprotonation, fast enough to allow the other steps of the catalytic cycle to influence the rate to a higher degree and obscure any differences in alkynylation rate. The unsubstituted phenylacetylene shows elements of both the behaviors of the electron-donating and electron-poor phenylacetylenes: It shows a dependence on the nature of the base, with quinuclidine again promoting the reaction rate to the greatest extent, although the effect on the reaction rate by TEA and DIPEA is reversed. This outcome can be seen for the NO_2-substituted phenylacetylene as well and possibly reflects the minor increase in basicity of DIPEA relative to TEA. Moreover, for TEA and for the low concentration reaction with DIPEA, the reaction rate of the unsubstituted phenylacetylene is slower than that of both the electron-poor and electron-rich phenylacetylenes. This behavior is in accordance with the Hammett correlation study. However, for the other set of reactions with the unsubstituted phenylacetylene the conversion is in between that of the electron-poor and electron-rich phenylacetylene. This could indicate that the changeover in mechanism may occur at different values for the Hammett substituent constant depending on the nature of the base, or that both mechanisms operate simultaneously for some substrates.

Kinetic Isotope Effects (KIE). To test whether or not the acetylenic carbon−hydrogen bond is broken in a reaction step strongly influencing the reaction rate, a KIE study was performed. Furthermore, to substantiate the mechanistic changeover hypothesis based on the Hammett correlation studies, the KIE was studied for phenylacetylene and the corresponding *para*-substituted nitro and dimethylamino analogues. The KIE was obtained by measuring the progress of the cross-coupling of normal and deuterated phenylacetylenes by UV−vis spectroscopy followed by a fit of an exponential expression to the data in the same manner as in the Hammett studies.

Proton exchange between phenylacetylenes and methanol is a relatively fast process under the reaction conditions employed. This process was utilized in the preparation of the deuterated samples. The normal phenylacetylene was used in the preparation of the stock solution for the measurements of the cross-coupling rate for both the normal and the deuterated phenylacetylene. Thus, a stock solution prepared from normal phenylacetylene, 4-iodobenzotrifluoride, base, and ligand in chlorobenzene was added in small aliquots to two separate cuvettes containing either regular or deuterated methanol. Leaving the cuvettes overnight ensured complete proton for deuterium exchange according to NMR spectroscopy. As a

(40) Krüger, H.; van Eldik, R. *J. Chem. Soc., Chem. Commun.* **1990**, 330.
(41) Gosling, R.; Tobe, M. L. *Inorg. Chem.* **1983**, *22*, 1235.
(42) Tobe, M. L. In *Comprehensive Coordination Chemistry*, 1 ed.; Wilkinson, G., Ed.; Pergamon: Oxford, 1987; Vol. 1, Chapter 7.
(43) Fox, A.; Hartman, J. S.; Humphries, R. E. *J. Chem. Soc., Dalton Trans.* **1982**, 1275.
(44) Seligson, A. L.; Trogler, W. C. *J. Am. Chem. Soc.* **1991**, *113*, 2520.
(45) Shaik, S. S. *J. Am. Chem. Soc.* **1981**, *103*, 3692.
(46) Shaik, S. S. *Prog. Phys. Org. Chem.* **1985**, *15*, 197.
(47) Pross, A. *Adv. Phys. Org. Chem.* **1985**, *21*, 99.
(48) de Meijere, A.; Chaplinski, V.; Gerson, F.; Merstetter, P.; Haselbach, E. *J. Org. Chem.* **1999**, *64*, 6951.
(49) Aue, D. H.; Webb, H. M.; Bowers, M. T. *J. Am. Chem. Soc.* **1976**, *98*, 311.

consequence, the KIE experiments had to be run in CH_3OH or CH_3OD depending on the isotope of interest. However, although reproducible in magnitude, it turned out to be difficult to obtain KIE values with high accuracy. This was mainly due to the sensitivity of the very dilute reactions, required for the UV measurements.

The result for the nitro-substituted phenylacetylene is consistent with a primary isotope effect, i.e., a k_H/k_D of around 2. For the dimethylamino-substituted analogue a much smaller isotope effect ($k_H/k_D \approx 0.9$) was seen (see the Supporting Information). The small inverse KIE could be explained by a small inverse solvent isotope effect due to differential solvation. Situated at the crossover point between the anionic and cationic pathway in the Hammett plot is the unsubstituted phenylacetylene, which was, therefore, expected to have an isotope effect somewhere in the range 0.9−2. Interestingly, a KIE value of around 2 was observed for this substrate as well.

The substantial KIE observed for the EWG substrate supports the assumption of a rate-influencing C−H bond breaking. Furthermore, the significant difference between the KIE observed for the EWG and the EDG-substituted phenylacetylenes, respectively, corroborates a mechanistic changeover as indicated by the Hammett plot.

Conclusion

There is a mechanistic changeover for the copper-free Sonogashira cross-coupling of *para*-substituted phenylacetylenes with 4-iodobenzotrifluoride when going from electron-poor to electron-rich alkynes. The changeover point is dependent on the nature of the amine base and its concentration. The preferred pathway for electron-rich alkynes is hypothesized to include a slow formation of a cationic Pd−alkyne complex, via an iodide−amine exchange. This proposition is supported by the negative slope of the Hammett plot for the EDG-substituted alkynes and the increasing reaction rate with increasing nucleophilicity of the applied amine. The electron-poor alkynes are hypothesized to react via a pathway in which the key step is proton transfer from an uncharged complex to produce the Pd−acetylide intermediate. This is corroborated by the positive slope of the Hammett plot for EWG-substituted alkynes and the primary isotope effect observed.

The practical implication is primarily that in copper-free Sonogshira couplings the optimum choice of base might differ substantially with substrate. Furthermore, the mechanistic insights might have implications in future developments of the copper-free Sonogashira coupling such as ligand design and choice of reaction media.

Experimental Section

General Procedure for the Preparation of α-Halostilbenes 6a−d. Silica gel 60 (5 g; equilibrated with the atmosphere at 120 °C for 48 h), 1-(2-phenylethynyl)-4-(trifluoromethyl)benzene (**5**) (49 mg, 2.0 mmol), and CH_2Cl_2 (10 mL) were placed in a 25 mL side-necked round-bottomed flask. HX precursor PX_3 (X = I, Br; 1.6 mmol) was added carefully to this suspension, and the flask was stoppered. The resulting suspension was stirred for 5 days at room temperature. The reaction was monitored by HPLC until consumption of the alkyne. The solution was filtered, and the filtrand washed repeatedly with CH_2Cl_2. The organic layer was washed with Na_2CO_3 solution (and additionally with $Na_2S_2O_3$ solution for the iodo compounds) and brine and dried over Na_2SO_4. The solvent was evaporated to obtain *E*/*Z* α-halostilbenes **6a−d**, which were purified by chromatography on silica gel with hexane as the eluant.

In the case of **6b**, where the yield was particularly low, an isomerization of **6a** to **6b** was done separately by stirring **6a** with 1 equiv of PI_3 over silica in CH_2Cl_2 for 5 days. Workup as described above gave the desired isomer **6b** in 15% yield.

(*E*)-1-Iodo-1-phenyl-2-(4-trifluoromethylphenyl)ethene (6a): pale yellow crystalline solid from diethyl ether/petroleum ether in 50% yield, mp 68−69 °C. ^{1}H NMR ($CDCl_3$): δ 7.44 (s, 1H vinylic), 7.36 (d, 2H, J = 8.3 Hz), 7.29 (m, 5H), 7.01 (d, 2H, J = 8.3 Hz) ppm. ^{13}C NMR ($CDCl_3$): δ 142.61, 140.60 (q, ^5J = 1.4 Hz), 140.04, 129.07, 129.02 (q, ^2J = 32.7 Hz), 128.99, 128.97, 128.68, 125.29 (q, ^3J = 3.8 Hz), 124.15 (q, ^1J = 272 Hz), 101.57 ppm. Anal. Calcd for $C_{15}H_{10}F_3I$: C 48.11, H, 2.67. Found: C 48.19, H 2.74.

(*Z*)-1-Iodo-1-phenyl-2-(4-trifluoromethylphenyl)ethene (6b): pale yellow, thick viscous liquid in 5% yield. ^{1}H NMR ($CDCl_3$): δ 7.68 (m, 4H), 7.59 (m, 2H), 7.29−7.41 (m, 2H), 7.07 (s, 1H, vinylic) ppm. ^{13}C NMR ($CDCl_3$): δ 143.91, 142.37, 136.03, 129.30, 129.16, 128.85, 128.84 (q, ^2J = 32.7 Hz), 128.61, 125.39 (q, ^3J = 3.8 Hz), 124.30 (q, ^1J = 272 Hz), 105.92 ppm. HRMS (EI) calcd for $C_{15}H_{10}F_3I$ 373.9779, found 373.977. (**6b** was not sufficiently pure for elemental analysis; small amounts of the tolane starting material were present. The identity of the compound was however well established by ^{1}H NMR, ^{13}C NMR, HRMS, NOESY, and trapping experiments to form the fully characterized derivative **7b**. For 2D NMR spectra, see the Supporting Information.)

(*E*)-1-Bromo-1-phenyl-2-(4-trifluoromethylphenyl)ethene (6c): colorless, thick viscous liquid, which solidified on standing for long time, in 54% yield, mp 30−31 °C. ^{1}H NMR ($CDCl_3$): δ 7.38 (d, 2H, J = 8.2 Hz), 7.33 (m, 5H), 7.19 (s, 1H, vinylic), 7.06 (d, 2H, J = 8.2 Hz) ppm; ^{13}C NMR ($CDCl_3$): δ 139.62 (q, ^5J = 1.4 Hz), 139.07, 131.81, 129.45, 129.35 (q, ^2J = 32.7 Hz), 129.23, 129.04, 129.00, 126.22, 125.37 (q, ^3J = 3.8 Hz), 124.15 (q, ^1J = 272 Hz) ppm. Anal. Calcd for $C_{15}H_{10}F_3Br$: C 55.04, H 3.06. Found: C 55.19, H 3.12.

(*Z*)-1-Bromo-1-phenyl-2-(4-trifluoromethylphenyl)ethene (6d): white crystalline solid from diethyl ether/petroleum ether in 25% yield, mp 56−57 °C. ^{1}H NMR ($CDCl_3$): δ 7.80 (d, 2H, J = 8.2 Hz), 7.66 (m, 4H), 7.40 (m, 3H), 7.24 (s, 1H, vinylic) ppm. ^{13}C NMR ($CDCl_3$): δ 140.66, 140.01 (q, ^5J = 1.4 Hz), 129.90 (q, ^2J = 32.7 Hz), 129.64, 129.42, 128.72, 128.67, 128.02, 126.67, 125.35 (q, ^3J = 3.8 Hz), 124.28 (q, ^1J = 272 Hz) ppm. Anal. Calcd for $C_{15}H_{10}F_3Br$: C 55.04, H 3.06. Found: C 55.25, H 3.15.

General Procedure for the Oxidative Addition of α-Halostilbenes to Pd^0. CD_3OD (400 μL) and CH_3OH (100 μL) were introduced to an argon-flushed NMR tube sealed with a silicon-rubber septum. A solution of 1,3,5-tris(trifluoromethyl)benzene (internal standard) in CH_3OH (100 μL, 1 mM), a solution of a α-halostilbene in CH_3OH (200 μL, 5 mM), a solution of $AsPh_3$ in CH_3OH (100 μL, 20 mM), and Et_3N (14 μL, 100 equiv of one of **6a−d**) were introduced into an NMR tube, and a ^{19}F NMR spectrum was recorded of the reaction mixture. A sharp singlet for the CF_3 group was observed. A solution of $Pd_2dba_3 \cdot CHCl_3$ in chlorobenzene (200 μL, 2.5 mM) was added, and the NMR tube was shaken well. The colorless solution became pale yellow on addition of the palladium solution, thus indicating immediate formation of a palladium−triphenylarsine complex. ^{19}F NMR spectra were recorded at desired time intervals. The product formation during and after oxidative addition was monitored by the presence of the CF_3 signals with respect to the internal standard taken as δ = 0 ppm.

Typical Procedure for Trapping the C−Pd^{II}−X Intermediate Complex Formed *in Situ*. Compound **6b** (18 mg, 0.048 mmol) and phenylacetylene (4.9 mg, 0.048 mmol, 5.3 μL) was added to a stirred and thoroughly degassed solution of $Pd_2dba_3 \cdot CHCl_3$ (1.25 mg, 1.2×10^{-3} mmol), $AsPh_3$ (1.47 mg, 4.8×10^{-3} mmol), and NEt_3 (504 mg, 5 mmol, 0.7 mL) in methanol/chlorobenzene (5 mL, 4:1). The reaction mixture was heated under stirring at 50 °C for 2 h. The solvent was evaporated and the product extracted with

diethyl ether. The organic layer was washed with water and brine, and the solvent was evaporated to give the crude product **7b**, which was purified by column chromatography (SiO2, ether/petroleum ether, 2:98).

(*E*)-1-(1,4-Diphenylbut-1-en-3-yn-2-yl)-4-(trifluoromethyl) benzene (7a): obtained from **6a** or **6c** as a white crystalline solid in 95% yield, mp 74−75 °C; ^{1}H NMR ($CDCl_3$): δ 7.48 (m, 2H), 7.40 (m, 4H), 7.33 (m, 6H), 7.17 (d, J = 8.2, 2H), 7.12 (s, 1H, vinylic) ppm; ^{13}C NMR ($CDCl_3$): δ 139.90 (q, ^5J = 1.4 Hz), 137.41, 134.78, 131.88, 129.70, 129.39 (q, ^2J = 32.6 Hz), 129.19, 128.97, 128.71, 128.57, 128.53, 126.98, 125.27 (q, ^3J = 3.8 Hz), 124.25 (q, ^1J = 272 Hz), 123.24, 91.86, 91.38 ppm. Anal. Calcd for $C_{23}H_{15}F_3$: C 79.22, H 4.30. Found: C 79.18, H, 4.30.

(*Z*)-1-(1,4-Diphenylbut-1-en-3-yn-2-yl)-4-trifluoromethylbenzene (7b): obtained from **6b** or **6d** as a white crystalline solid in 80% yield, mp 94−95 °C. ^{1}H NMR ($CDCl_3$): δ 8.12 (d, J = 8.5 Hz, 2H), 7.81 (m, 2H), 7.67 (d, J = 8.1 Hz, 2H), 7.56 (m, 2H), 7.32−7.47 (m, 6H), 7.23 (s, 1H, vinylic) ppm. ^{13}C NMR ($CDCl_3$): δ 140.25 (q, ^5J = 1.4 Hz), 139.18, 132.96, 131.81, 129.85 (q, ^2J = 32.4 Hz), 129.35, 129.11, 128.81, 128.77, 128.66, 126.79, 125.41 (q, ^3J = 3.7 Hz), 124.38, 124.33 (q, ^1J = 272 Hz), 123.06, 98.17, 88.22 ppm. Anal. Calcd for $C_{23}H_{15}F_3$: C 79.22, H 4.30. Found: C 79.54, H 4.41.

General Procedure for the Competitive Hammett ^{19}F NMR Spectroscopic Experiments. CD_3OD (400 μL) and CH_3OH (100 μL) were introduced into an argon-flushed NMR tube sealed with a silicon septum. Et_3N (42 μL, 30 equiv of 4-iodobenzotrifluoride) and methanolic solutions of 4-iodobenzotrifluoride (100 μL, 100 mM), phenylacetylene (100 μL, 50 mM), substituted phenylacetylene (100 μL, 50 mM), and $AsPh_3$ (25 μL, 20 mM) were added to the tube. A ^{19}F NMR spectrum was recorded, and a sharp singlet for the CF_3 group was observed. A solution of $Pd_2dba_3 \cdot CHCl_3$ in chlorobenzene (50 μL, 2.5 mM) was added and shaken well. Single-scan ^{19}F NMR spectra were recorded at desired intervals of time. The amount of tolane products formed could be calculated by the integration of the CF_3 signals assuming equal relaxation times for the CF_3 groups.

General Procedure for the Absolute Hammett ^{19}F NMR Spectroscopic Experiments. The absolute rate Hammett experiments were performed as described for the competitive ones with the exception that 200 μL of the appropriate 50 mM stock solution of substituted phenylacetylene was used instead of 100 μL each of two different stock solutions.

General Procedure for the Preparation of the Tolane Reference Substances. 4-Ethynyl-α,α,α-trifluorotoluene (170.1 mg, 1 mmol, 163 μL) and the appropriately *para*-substituted bromobenzene (1 mmol) were placed in a two-necked pear-shaped 25 mL flask fitted with a reflux condenser. Freshly distilled NEt_3 was added, and the resulting solution was bubbled with argon for 10 min. $Pd_2(dba)_3 \cdot CHCl_3$ (12.9 mg, 0.0125 mmol), $HP(tBu)_3BF_4$ (7.3 mg, 0.025 mmol), and CuI (9.5 mg, 0.05 mmol) was added as solids under a gentle stream of argon. The temperature was raised to boiling point, and the reaction was allowed to gently reflux for 18 h. The solvent was evaporated and the resulting crude mixture triturated with petroleum ether (40−60) and passed through a short column of silica. After concentration and cooling, the product precipitated as white needles or sheets. Some tolanes were too soluble in petroleum ether or precipitated as a discolored powder. These crude mixtures were instead recrystallized from methanol.

Some of the tolanes are known, and our NMR data were in accordance with that described in the literature.[50–53] Moreover, ^{19}F NMR shifts for all tolanes relative to 4-iodobenzotrifluoride are given in Table S11 in the Supporting Information.

1-[(4-Chlorophenyl)ethynyl]-4-(trifluoromethyl) benzene: white crystalline sheets after recrystallization from MeOH in 90% yield, mp 116−117 °C. ^{1}H NMR ($CDCl_3$): δ 7.62 (s, 4H), 7.48 (d, ^3J = 8.7 Hz, 2H), 7.35 (d, J = 8.7 Hz, 2H). ^{13}C NMR ($CDCl_3$): δ 135.15, 133.16, 132.02, 130.35 (q, ^2J = 32.7 Hz), 129.05, 126.98 (q, ^5J = 1.4 Hz), 125.55 (q, ^3J = 3.8 Hz), 124.12 (q, ^1J = 272 Hz), 121.27, 90.78, 89.08 (q, ^6J = 0.8 Hz) ppm. Anal. Calcd for $C_{15}H_8ClF_3$: C 64.19, H 2.87. Found: C 64.04, H 2.94.

1-[(4-Nitrophenyl)ethynyl]-4-(trifluoromethyl)benzene: white crystalline solid in 67% yield, mp 110−111 °C. ^{1}H NMR ($CDCl_3$): δ 8.25 (d, ^3J = 8.9 Hz, 2H), 7.70 (d, J = 8.9 Hz, 2H), 7.66 (m, 4H). ^{13}C NMR ($CDCl_3$): δ 147.60, 132.71, 132.31, 131.13 (q, ^2J = 32.8 Hz), 129.63, 126.12 (q, ^5J = 1.4 Hz), 125.71 (q, ^3J = 3.8 Hz), 123.98 (q, ^1J = 272 Hz), 123.94, 93.01 (q, ^6J = 0.8 Hz), 89.74 ppm. Anal. Calcd for $C_{15}H_8F_3NO_2$: C 61.86, H 2.77. Found: C 61.94, H 2.82.

1-[(4-Acetophenyl)ethynyl]-4-(trifluoromethyl)benzene: white crystalline needles in 88% yield, mp 122−123 °C. ^{1}H NMR ($CDCl_3$): δ 8.25 (d, ^3J = 8.3 Hz, 2H), 7.60−7−68 (m, 6H). ^{13}C NMR ($CDCl_3$): δ 197.33, 136.81, 132.12, 132.02, 130.55 (q, ^2J = 32.8 Hz), 128.47, 127.49, 126.64 (q, ^5J = 1.4 Hz), 125.52 (q, ^3J = 3.8 Hz), 124.02 (q, ^1J = 272 Hz), 91.13 (q, ^6J = 0.8 Hz), 90.95, 26.74 ppm. Anal. Calcd for $C_{17}H_{11}F_3O$: C 70.83, H 3.85. Found: C 70.76, H 3.92.

General Procedure for the Base−Substrate Correlation Studies. The screening was performed by a series of reaction carousel experiments. In each series 12 reactions on a 4 mL scale were performed simultaneously. A stock solution (A) of the appropriate phenylacetylene (0.88 mmol), $AsPh_3$ (1.96 mg, 6.4 × 10^{-3} mmol), 4-iodobenzotrifluoride (217.6 mg, 0.8 mmol), and 1,3,5-tris(trifluoromethyl)benzene (37.6 mg, 0.133 mmol) in chlorobenzene was prepared in a 5 mL volumetric flask. For higher accuracy, $AsPh_3$ was added to this stock solution as a 0.2 mL aliquot from another stock solution (B) made up from $AsPh_3$ (98 mg, 0.32 mmol) in chlorobenzene (10 mL). The base (0.4 mmol for 100 mM experiments and 1.6 mmol for 400 mM experiments) and an aliquot of stock solution A (0.25 mL) giving R-phenylacetylene (0.044 mmol), $AsPh_3$ (0.098 mg, 3.2 × 10^{-4} mmol), 4-iodobenzotrifluoride (10.9 mg, 0.04 mmol), and 1,3,5-tris(trifluoromethyl)benzene (1.9 mg, 0.007 mmol) were introduced into the reaction tube and were diluted with MeOH to 4 mL. Argon presaturated with MeOH was bubbled through each reaction mixture for 5 min, and then a vacuum/argon cycle was carried out. A stock solution of $Pd_2dba_3 \cdot CHCl_3$ (8.3 mg, 0.008 mmol) in degassed chlorobenzene (25 mL) was made up, and an aliquot (0.25 mL, 8 × 10^{-5} mmol) was added to each reaction tube via syringe. This gave a catalyst loading of 0.4 mol% with a $AsPh_3$:Pd^0 ratio of 2:1. A stock solution of 1,2-bis(diphenylphosphino)ethane (dppe) (159.4 mg, 0.4 mmol) in toluene (5 mL) was prepared. After 1 h the reaction was quenched with an aliquot of the dppe solution (0.2 mL, 0.016 mmol; 100 equiv excess relative to Pd) in the identical order to the addition of the Pd solution. ^{19}F NMR spectroscopic analysis was carried out for each reaction mixture, and the amount of product formed could be calculated by the integration of the CF_3 peak.

Studies of the Kinetic Isotope Effect. Procedure for determining the kinetic isotope effect by UV−vis spectroscopy: In a 5 mL volumetric flask, $AsPh_3$ (7.66 mg, 0.025 mmol), 4-iodobenzotrifluoride (0.136 g, 0.5 mmol), R-phenylacetylene (0.5 mmol), and Et_3N (0.7 mL, 508.2 mg, 5 mmol, 10 equiv) were introduced and diluted with chlorobenzene to give a stock solution. For the UV−vis experiment, CH_3OH (240 μL) and CD_3OD (240 μL) were introduced into two separate 1 mm cuvettes flushed with argon and fitted

(50) Liang, B.; Dai, M.; Chen, J.; Yang, Z. *J. Org. Chem.* **2005**, *70*, 391.

(51) Mouriès, V.; Waschbüsch, R.; Carran, J.; Savignac, P. *Synthesis* **1998**, 271.

(52) Johnson, S. A.; Liu, F.-Q.; Suh, M. C.; Zürcher, S.; Haufe, M.; Mao, S. S. H.; Tilley, T. D. *J. Am. Chem. Soc.* **2003**, *125*, 4199.

(53) Alonso, D. A.; Nájera, C.; Pacheco, M. C. *Adv. Synth. Catal.* **2003**, *345*, 1146.

with tight silicon rubber septum, and the stock solution (12.5 μL) was added. The cuvettes were left overnight to ensure complete conversion to deuterioacetylene. The instrument was set to zero absorption. A solution of $Pd_2dba_3 \cdot CHCl_3$ in chlorobenzene (6.25 μL, 2.5 mM, 2.5 Pd mol %) was added and shaken well. The product formation in the reaction was monitored by the amount of absorption at $\lambda_{max} = 350$ nm for NO_2, 282 nm for H, and 368 nm for NMe_2.

Acknowledgment. Financial support from AstraZeneca R&D Mölndal and the Swedish Research Council is gratefully acknowledged.

Supporting Information Available: Materials and instrumentation. An account of the results from the carbopalladation study together with typical ^{19}F NMR spectra. Computational methods and results. Deduction of rate equations. Hammett studies, initial reaction rates, and ^{19}F NMR shifts for the resulting tolanes. Procedure for the base concentration study and product yields for the reaction carousel experiments designed to demonstrate the effect of nature and concentration of base. Kinetic traces and measured KIEs. ^1H NMR, ^{13}C NMR, NOESY, and COSY spectra. This material is available free of charge via the Internet at http://pubs.acs.org.

OM800251S